# Inertial Oscillations due to a Moving Front

PIJUSH K. KUNDU

*Oceanographic Center, Nova University, Dania, FL 33004*

RICHARD E. THOMSON

*Institute of Ocean Science, Sidney, B.C. V8L 4B2, Canada*

(Manuscript received 8 January 1985; in final form 8 April 1985)

## ABSTRACT

A solution for a concentrated line front translating at speed $U$ is given. It is shown that the frequency is near-inertial if $U \gg c_1$, where $c_1$ is the long internal wave speed of the first baroclinic mode. Each mode has a characteristic frequency $\omega_n$ associated with it. The spectra contain a near-inertial primary peak, composed of the higher modes, whose blue shift increases with depth. They also contain secondary peaks at higher internal wave frequencies if $U$ is only slightly larger than $c_1$. The flow field is intermittent, and involves a continuous interchange of energy between the surface layer and the stratified interior. The dominant period of this intermittency is the beating period of the first mode with a purely inertial oscillation. Short periods of apparent subinertial motion are also generated. Several features of the solution are in agreement with observation.

## 1. Introduction

The passage of storms and their associated fronts can generate large inertial oscillations in the surface layer and in the thermocline. Aspects of this phenomenon have been demonstrated in several models. Geisler (1970) constructed a two-layer analytical model of the response to a moving storm, and showed that the nature of the solution depends on the relative magnitudes of its speed of translation $U$ and the long internal wave speed $c_n$. For common oceanographic parameter values the baroclinic modes satisfy $U > c_n$, for which the equations of motion are hyperbolic and the solution has a spreading wake that decays with the downstream distance approximately as $x^{1/2}$. The barotropic mode satisfies $U < c_n$, for which the system is elliptic and gives a symmetric response with no wake. The corresponding problem in a stratified ocean was studied numerically by Price (1983). Gill (1984) studied the adjustment of a current in the surface layer, left behind by a rapidly propagating storm, through the radiation of inertio-gravity waves. Rubenstein (1983) numerically studied the vertical propagation in a stratified fluid forced by a wind stress periodic in space and impulsive in time.

The purpose of this note is to give a simple solution for the flow field due to a moving front in the form of a concentrated (delta-function) line source, and examine the behavior of the resulting scale, spectra, amplitude, and vertical propagation. The major results are that the spectra may have multiple peaks, the blue shift of the primary peak increases with depth,

and that the flow field is intermittent due to a beating phenomenon. It will be seen that the present simple model contains many of the features of solutions of Gill (1984) and Rubenstein (1983), although their models do not consider propagating storms. Some aspects of the solution are then compared to observations near the coast of British Columbia.

## 2. Solution for a concentrated front

Consider a front aligned in the $y$-direction and moving in the $x$-direction at speed $U$. The ocean has a stratified interior with buoyancy frequency $N(z)$, a surface mixed layer of thickness $h$ where $N(z) = 0$, and a flat bottom at $z = -D$. For long fronts the response can be assumed independent of $y$, and the linearized inviscid equations of motion are

$$\left.\begin{aligned} u_t - fv &= -p_x + F \\ v_t + fu &= G \\ u_x + w_z &= 0 \\ \rho_t - N^2 w/g &= 0 \\ p_z + \rho g &= 0 \end{aligned}\right\} \quad (1)$$

where the variables have their usual meaning. The stress is assumed to enter the ocean as a body force in the mixed layer. Consequently $(F, G) = (\tau^x/h, \tau^y/h)$ in the surface layer, and $(F, G) = (0, 0)$ below. Boundary conditions are

$$w = 0 \quad \text{at} \quad z = 0, -D. \quad (2)$$

Solutions to (1)–(2) can be found by expanding the variables in terms of the normal modes $\phi_n(z)$ of the system:

$$(u, v, p) = \sum_{n=0}^{\infty} (u_n, v_n, p_n)\phi_n,$$

$$w = \sum_{n=0}^{\infty} w_n \int_{-D}^{z} \phi_n dz, \quad p = \sum_{n=0}^{\infty} p_n\phi_{nz}. \quad \Biggr\} \quad (3)$$

The eigenfunctions satisfy

$$\left(\frac{\phi_{nz}}{N^2}\right)_z + \frac{1}{c_n^2} \phi_n = 0 \quad (4)$$

subject to $\phi_{nz} = 0$ at $z = 0, -D$, where $c_n$ represent the long internal wave speed of the mode. The modal coefficients satisfy

$$u_{nt} - fv_n + p_{nx} = \tau_n^x$$
$$v_{nt} + fu_n = \tau_n^y \quad \Biggr\} \quad (5)$$
$$p_{nt} + c_n^2 u_{nx} = 0$$

where the forcing coefficients are given by

$$(\tau_n^x, \tau_n^y) = (\tau^x, \tau^y) \Bigg/ \int_{-D}^{0} \phi_n^2 dz. \quad (6)$$

The equation for $u_n$ alone obtained from (5) is

$$(\partial_{tt} + f^2)u_n - c_n^2 u_{nxx} = \tau_{nt}^x + f\tau_n^y. \quad (7)$$

A coordinate system fixed with the front is now adopted. After the initial transients have died away, the field is steady in the moving frame of reference; this would happen in a time in which the gravity waves have crossed the width of the storm, typically several hours. The equations of motion in the moving coordinate system can be written by replacing $\partial_t$ with $-U\partial_x$ in (7). Equation (7) then gives

$$u_{nxx} + k_n^2 u_n = \frac{-U\tau_{nx}^x + f\tau_n^y}{U^2 - c_n^2} \quad (8)$$

where

$$k_n = \frac{f/U}{(1 - c_n^2/U^2)^{1/2}}. \quad (9)$$

For typical oceanographic parameters the barotropic mode satisfies $U < c_n$, for which (8) has solutions that decay exponentially away from the source. The baroclinic modes on the other hand satisfy $U > c_n$ for which (8) has trigometric solution behind the front. The field in this case is required to vanish ahead of the front because it moves faster than the speed of propagation of information, namely the group velocity $c_n$ of short wavelengths. Equation (8) can be solved given the spatial distribution of the forcing function. For our purposes we shall choose

the simplest realistic form. A front is characterized by a sudden shift in the direction of the wind, with no large change in the magnitude (Thompson and Huggett, 1981a). A common pattern for a warm front would be a northeastward stress propagating eastward would be a northeastward stress ahead of the front and an eastward stress behind it. Assuming that $\tau^x$ and $\tau^y$ are of similar magnitude, the ratio of the two forcing terms in the numerator of (8) is $R = U/f\Delta x$, where $\Delta x$ is the thickness of the front. Typical values are $U \sim 500$ cm s$^{-1}$, $f \sim 10^{-4}$ s$^{-1}$ and $\Delta x \sim 10$ km, giving $R \sim 5$. The forcing term involving $\tau^y$ is therefore neglected in (8).

If $\tau^x$ drops by $\tau_0$ across the front, then

$$\tau_x^x = -\tau_0\delta(x) \quad (10)$$

where $\delta(x)$ is the Dirac delta function. Therefore

$$\tau_{nx}^x = -\tau_{0n}\delta(x) \quad (11)$$

where, by (6),

$$\tau_{0n} = \tau_0 \Bigg/ \int_{-D}^{0} \phi_n^2 dz. \quad (12)$$

Equation (8) then becomes

$$u_{nxx} + k_n^2 u_n = \frac{U\tau_{0n}\delta(x)}{U^2 - c_n^2}. \quad (13)$$

### Baroclinic solution

In this case $U > c_n$, and $k_n$ is real. The solution of (13) satisfying the radiation boundary condition of $u_n = 0$ for $x > 0$ is

$$u_n = \frac{U\tau_{0n}}{(U^2 - c_n^2)k_n}\left[\sin k_n x \int_{\infty}^{x} \cos k_n x \delta(x)dx\right.$$

$$\left. - \cos k_n x \int_{\infty}^{x} \sin k_n x \delta(x)dx\right]. \quad (14)$$

which simplifies to

$$u_n = -\frac{\tau_{0n} \sin k_n x}{f(1 - c_n^2/U^2)^{1/2}}, \quad x \leq 0. \quad (15)$$

### Barotropic solution

In this case $U < c_0$, and (13) is rewritten as

$$u_{0xx} - K_0^2 u_0 = \frac{U\tau_{00}\delta(x)}{U^2 - c_0^2}, \quad (16)$$

where

$$K_0 = \frac{f/c_0}{(1 - U^2/c_0^2)^{1/2}}.$$

The solution to (16) is

$$u_0 = Ae^{K_0 x} + Be^{-K_0 x} + \frac{U\tau_{00}}{2K_0(U^2 - c_0^2)}$$

$$\times \left[e^{K_0 x} \int_{\infty}^{x} e^{-K_0 x}\delta(x)dx - e^{-K_0 x}\int_{-\infty}^{x} e^{K_0 x}\delta(x)dx\right].$$

$$(17)$$

Since $u_0$ is bounded at $x = \pm\infty$, the constants must be $A = B = 0$. Equation (17) then reduces to

$$u_0 = \frac{U\tau_{00}e^{-K_0|x|}}{2fc_0(1 - U^2/c_0^2)^{1/2}}, \quad \text{all} \quad x. \quad (18)$$

Equations (15) and (18) constitute the baroclinic and barotropic contributions to the velocity field, and the complete solution is obtained in the next section by summing over a large number of modes. The series (15) converges slowly, the convergence being faster for thicker mixed layers. It is clear that the barotropic contribution (18) is small since $c_0 \gg U$. The characteristics of the flow field are therefore dominated by the baroclinic contribution (15).

Note in (15) that the wake due to a *line* source does not decay, whereas that due to a *point* source is in the form of a Bessel function which decays away from the source (Geisler, 1970). This is because the wake due to a point source widens downstream, and its strength consequently diminishes roughly as $x^{1/2}$.

From (9) and (15) the wavelength for a mode is found to be

$$\lambda_n = \frac{2\pi U}{f}(1 - c_n^2/U^2)^{1/2} = \lambda_i(1 - c_n^2/U^2)^{1/2}. \quad (19)$$

The wavelength that gives exactly the inertial period in the fixed frame is $\lambda_i = 2\pi U/f$, which will be referred to as the "inertial wavelength". Equation (19) shows that $\lambda_n \approx \lambda_i$ for $c_n \ll U$. The exact period of the mode in the fixed frame is

$$t_n = \frac{\lambda_n}{U} = \frac{2\pi}{f}(1 - c_n^2/U^2)^{1/2} = t_i(1 - c_n^2/U^2)^{1/2}$$

where $t_i = 2\pi/f$ is the inertial period. The frequency of a mode is therefore

$$\omega_n = \frac{f}{(1 - c_n^2/U^2)^{1/2}} \quad (20)$$

which is near-inertial only if $c_n \ll U$. Since $c_n$ increases with $N$ and $D$, the blueshift for a particular mode increases with an increase of the stratification or depth.

Equation (20) can be derived more simply as follows (J. P. McCreary, private communication, 1984). The allowed frequencies are the points of intersection of the gravity wave dispersion relation $\omega_n^2 = f^2 + c_n^2 k^2$ with the straight line $Uk - \omega_n = 0$, the latter representing the transformation $U\partial_x + \partial_t = 0$. Elimination of $k$ gives (20).

The limiting cases of the solution for slow and fast propagation speeds are of interest. For $U \to 0$, all modes behave like the barotropic mode (18), which reduces to $u_n = U\tau_{0n} \exp(-f|x|/c_n)/2fc_n$. In the opposite extreme of a very fast storm, all modes (including the barotropic) behave according to (15). Then it follows from (9), (15), and (3) that the velocity field is

$$u = -f^{-1}\sin(fx/U)\sum_{n=0}^{\infty}\tau_{0n}\phi_n,$$

which gives

$$u = -\frac{\tau_0}{fh}\sin\left(\frac{fx}{U}\right), \quad x \leqslant 0 \quad (21)$$

in the surface layer, and $u = 0$ below. The frequency of the oscillations is then almost exactly inertial. A more realistic fast storm is, however, one for which $U \gg c_n$ for the baroclinic modes but $U \ll c_0$. For this case it is easy to show that

$$u = -f^{-1}\sin(fx/U)\sum_{n=1}^{\infty}\tau_{0n}\phi_n,$$

which gives

$$u = -\frac{\tau_0(1 - h/D)}{fh}\sin\left(\frac{fx}{U}\right), \quad x \leqslant 0 \quad (22)$$

in the surface layer, and the smaller slab-like compensating value of $u = \tau_0 \sin(fx/U)/fD$ below.

It is shown in the next section that several interesting features can be illustrated by evaluating the velocity field due to a line source. The characteristics of the solution will be valid as long as the front is thin compared to the relevant length scale, namely $\lambda_1$. This criterion is easily satisfied for typical oceanographic parameters, in which $\lambda_1$ is several hundred kilometers. Besides, the solution due to a distributed forcing function in (8) (including a nonzero $\tau^y$) can be constructed easily by replacing $-\tau_{0n}\delta(x)$ in (14) and (17) by a general distribution $X(x) \equiv \tau_{nx}^x - f\tau_n^y/U$.

## 3. Evaluation of solution

The following parameters appropriate for a continental shelf are assumed for the numerical evaluation of the standard case discussed in the paper:

$D = 250$ m
$h = 25$ m
$N = 10^{-2}$ s$^{-1}$
$U = 150$ cm s$^{-1}$
$\tau_0 = 1$ dyn cm$^{-2}$
$f = 10^{-4}$ s$^{-1}$

The mode shapes $\phi_n(z)$ are generated by solving the eigenvalue problem (4). The first three eigenvalues are found to be $c_1 = 78$ cm s$^{-1}$, $c_2 = 39$ cm s$^{-1}$ and $c_3 = 26$ cm s$^{-1}$. The barotropic mode is taken to be $\phi_0 = 1$ and $c_0 = \sqrt{gD} = 5000$ cm s$^{-1}$. Modal coefficients $u_n$ are found from (15) and (18), and 50 modes are summed in (3) to obtain the velocity field $u(x, z)$.

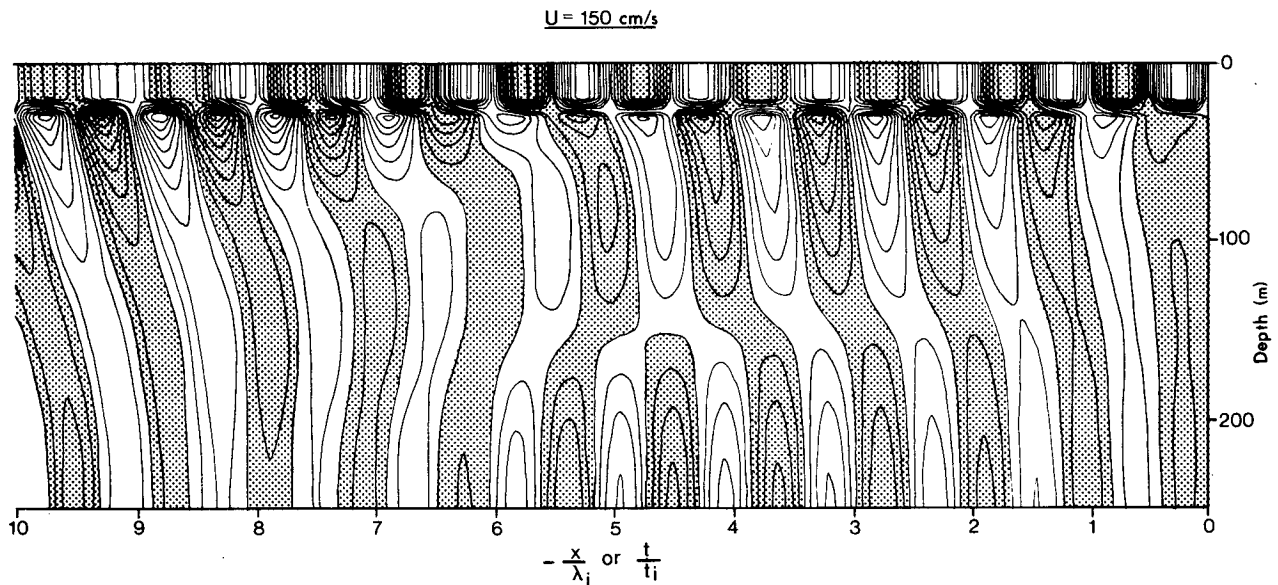Figure 1 shows the contour plot of $u$, where the concentrated front is at $x = 0$. The horizontal axis

U = 150 cm/s



FIG. 1. Contours of $u$ due to a concentrated front located at $x = 0$ and moving at $U = 150$ cm s$^{-1}$. Contour interval is 0.4 cm s$^{-1}$. Negative region is shaded. The horizontal axis is either (distance)/(inertial wavelength) in the moving frame, or (time)/(inertial period) in the fixed frame. Note the upward phase propagation associated with downward energy propagation, the dominant $5.8t_i$ periodicity, and clear evidence of the first mode in the range $3t_i < t < 5t_i$.

represents the distance in the moving coordinate system, or the time in the fixed coordinate system. Notice that the frequency near the bottom is higher than that in the mixed layer. The constant phase lines therefore gradually lean over and produce an upward phase propagation throughout the water column up to $5t_i$. This is associated with a downward energy propagation from the mixed layer. Beyond $5t_i$ there is some downward phase propagation in the bottom half, signifying a bottom reflection of energy.

The frequency shifts for the first three baroclinic modes are found from (20) to be 17.1%, 3.65% and 1.55% above inertial, respectively. Initially all the modes are nearly in phase in the mixed layer. The first mode, however, oscillates at a rate 17.1% higher than the inertially oscillating high order modes, and therefore becomes 90° out of phase in a time $(\pi/2(\omega_1 - f)$ Gill, 1984. The first mode then makes its presence felt completely below the mixed layer, and the energy in the mixed layer decreases by an amount corresponding to its energy. Such outfluxes of energy cause the loss of mixed layer energy evident in Fig. 1.

In a time $2\pi/(\omega_1 - f) = 5.8t_i$, the first mode again becomes in phase with the higher modes in the mixed layer; a new set of contour lines then re-emerge out of the mixed layer as the first mode starts to become out of phase once again. The energy therefore oscillates with a period $5.8t_i$ due to a constant interchange of energy (upward and downward) between the mixed layer and the deeper water (Gill, 1984). This phenomenon seems to be partly responsible for the observed

intermittency of inertial oscillations, although other mechanisms like random forcing (Kundu, 1984) can also cause intermittency. Rubenstein (1983) also noticed this continuous interchange of energy between the mixed layer and the stratified interior. [Rubenstein did not study a propagating front problem, but the surface forcing by a stationary wind impulsive in time and periodic in space with wavenumber $k$. It can be shown that his numerical solutions should be formally same as ours if his $(1 + c_n^2 k^2/f^2)$ is replaced by our $(1 - c_n^2/U^2)^{-1}$.]

The $5.8t_i$ periodicity not only occurs in the amplitudes but also in the phases of the oscillations; the "phase" here is defined as $\theta(t)$ in $u = u_0 \cos(ft + \theta)$. This is shown in a plot of the amplitude and phase of the solution at three depths (Fig. 2), found by complex demodulation at the inertial frequency. The generally upward trend of the phase signifies that the frequency is superinertial. The mean slope of the phase gives the "blue shift" to be 0.4% in the mixed layer, 2.2% at 90 m, and much higher at the bottom, where it is difficult to estimate because of the severe oscillation of the phase. The blue shift therefore increases with depth, a conclusion previously reached by Kundu et al. (1983) in a coastal model, and can also be seen in the hurricane calculations of Price (1983). The reason for this is the fact that the higher frequencies (lower modes) disperse earlier from the mixed layer.

Amplitudes in Fig. 2 show that up to $t = 10t_i$ the subsurface maxima occur later than the surface minima, the time lag increasing with depth. This is due
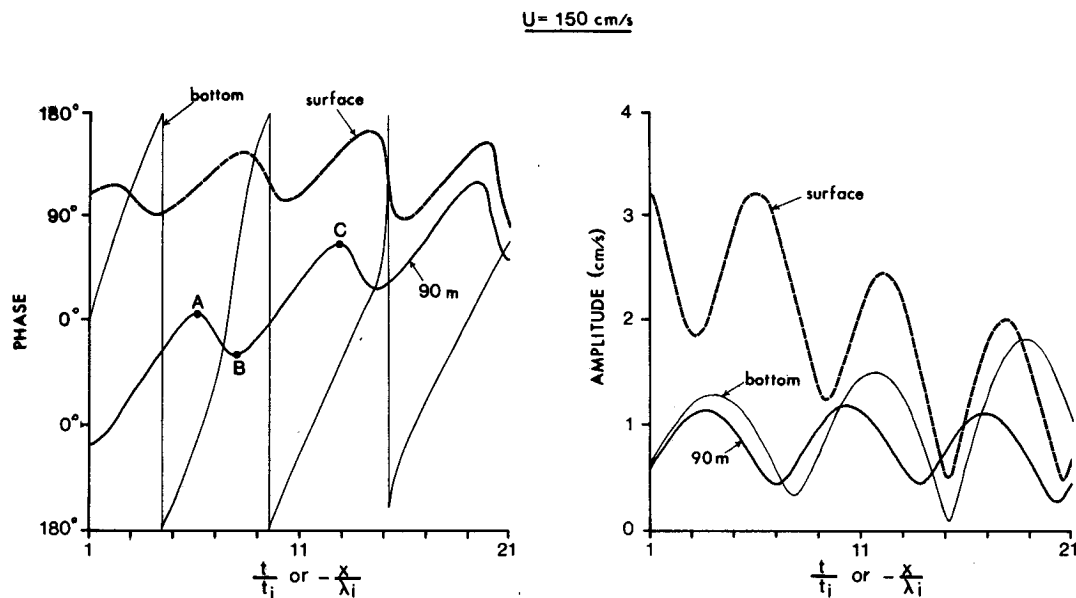
FIG. 2. Amplitude and phase at inertial frequency at three depths found by complex demodulation. The speed of the front is $U = 150$ cm s$^{-1}$. Note the dominant $5.8t_i$ periodicity of both the amplitude and phase, and the generally increasing trend of the phase signifying superinertial frequency. The frequency increases with depth. The time axis starts at $t = t_i$ because of the loss of record length by the demodulation filter.

to a downward propagation of energy from the surface at a finite group speed. The vertical group speed estimated from the time lag at the bottom is 0.5 cm s$^{-1}$, which agrees with the expression for vertical group speed found from the dispersion relation

$$c_{gz} = \frac{(\omega^2 - f^2)^{3/2}}{\omega k N}$$

on substitution of $\omega = 1.17f$ and $k = f/U$.

The superposition of the $5.8t_i$ periodicity on the mean trend of the phase means that the latter sometimes increases (segment BC in Fig. 2) and sometimes decreases (segment AB) with time. This feature is also seen in the solution of Gill (1984; his Fig. 7). The interval of time corresponding to these *apparent* subinertial frequencies corresponding to AB are, however, no more than two inertial periods long, and do not generate a subinertial spectral peak, as will be seen later. It is nevertheless curious that short apparent subinertial motions are generated although all the modes have frequencies $\omega_n > f$. Such occasional subinertial frequencies are frequently observed in current measurements (Kundu, 1976b; Thomson and Huggett, 1981a).

On the other hand, the intervals such as BC add up to a large fraction of the time series, and *additional* spectral peaks are therefore expected. In other words, the spectra should have multiple peaks, and this is indeed the case (Fig. 3). The spectra at all three depths have a double peak, one corresponding to the

mean trend of the phase and the other corresponding to time segments such as BC. Close inspection of Fig. 3 shows that the second peak at all three depths occurs at $\omega/f = 1.17$, which corresponds exactly to that of the first mode. Bottom reflection has therefore established a standing first mode in the vertical, a fact especially evident in the subsurface flow between $t = 3t_i$ and $t = 5t_i$. A similar feature can also be noticed in Rubenstein's calculations.

The peaks due to the higher modes ($\omega_2 = 1.036f$, $\omega_3 = 1.015f$, $\cdots$) are not visible in Fig. 3, since they fall too close to one another. In fact, the blue-shifted primary peak is due to the second and higher modes which contribute significantly to the solution. The very high-order modes, with frequencies practically coincident with $f$, make a negligible contribution to the solution; that is why the primary peak is blue shifted.

It is apparent that the secondary peak corresponding to the first mode can be moved closer to the primary peak simply by increasing $U$. This is seen in Fig. 4a, which shows the bottom spectrum for $U = 500$ cm s$^{-1}$. In this case $\omega_1 = 1.012f$, and this is where the spectral peak in Fig. 4a occurs. This case satisfies $U \gg c_n$ for the baroclinic modes, and $U \ll c_0$. Such a limiting case has been examined in the previous section, for which the velocity field is given by (22) in the surface mixed layer and an oppositely directed slab motion underneath. The contours of $u$ (not shown) are now nearly vertical lines, showing little lags in phase or energy propagation. There is, however,
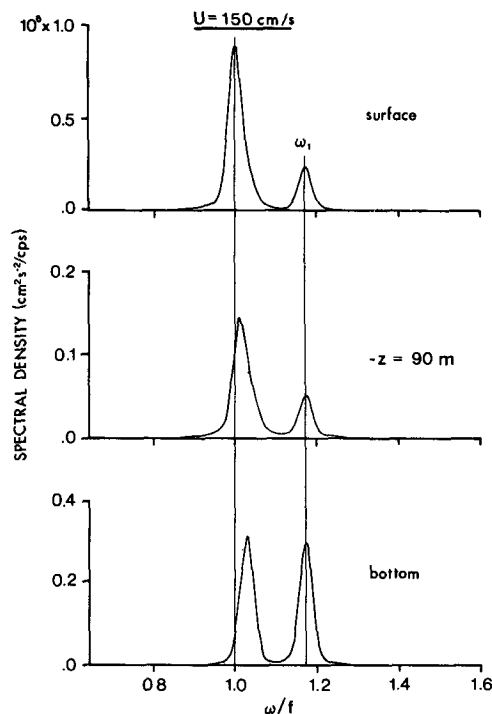
FIG. 3. High resolution spectra at three depths for a front moving at $U = 150$ cm s$^{-1}$. The record length is $40t_i$, the bandwidth is $0.004f$, and the degree of freedom is 4. The secondary peak coincides with the first mode frequency $\omega_1 = 1.17f$.



FIG. 4. Effect of changing the translation speed of front on the spectral characteristics. The bottom spectra are shown for $U = 100$ and $U = 500$ cm s$^{-1}$. Note that the spectral peaks corresponding to $\omega_1$ and $\omega_2$ are distinguishable for the slower front.

a slow decrease of the surface amplitudes and an increase in the subsurface amplitudes (Fig. 5).

In the opposite extreme of a slow front, with $U$ slightly larger than $c_1$, the spectral peaks corresponding to the first few modes are far apart and hence should be distinguishable. This is indeed the case, as a calculation with $U = 100$ cm s$^{-1}$ shows (Fig. 4b). Equation (20) now gives $\omega_1 = 1.60f$ and $\omega_2 = 1.086f$, and the spectral peaks corresponding to each of these are visible in Fig. 4b. Obviously peaks corresponding to more modes would be visible by taking $U$ further close to $c_1$. Note that noninertial internal waves (corresponding to the lower modes) are generated by slowly moving storms. These would contain a higher proportion of energy if the ocean has a thermocline, since then the convergence of the series (3) is faster. A calculation assuming that $N(z)$ has a thermocline indeed showed that the noninertial spectral peaks generated by slow storms were dominant.

## 4. Comparison with data

For comparison a front-forced event observed near the coast of British Columbia by Thomson and Huggett (1981a) will be reexamined. About 2–4 months of current meter data were collected at 10 stations during the summer of 1977. We will only
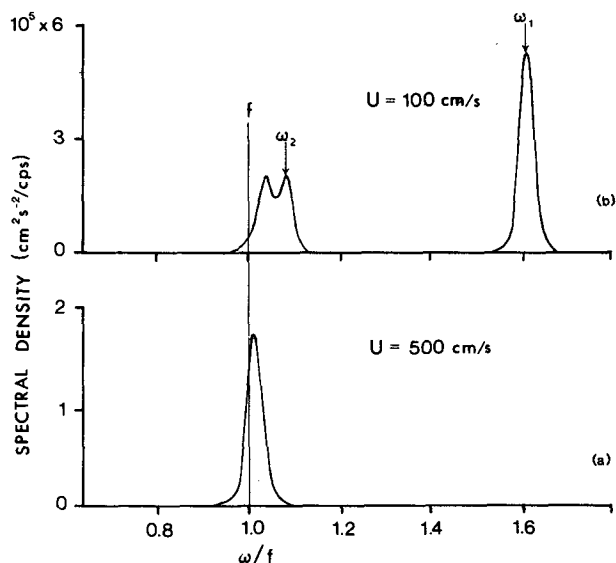
concern ourselves with the measurements in the surface layer, less than 25 m deep. The tides are removed by harmonic analysis, and the inertial oscillations are extracted by bandpass filtering around the inertial frequency. Two events of large inertial oscillations are observed during the period of measurements, one starting June 20 and the other starting August 21.
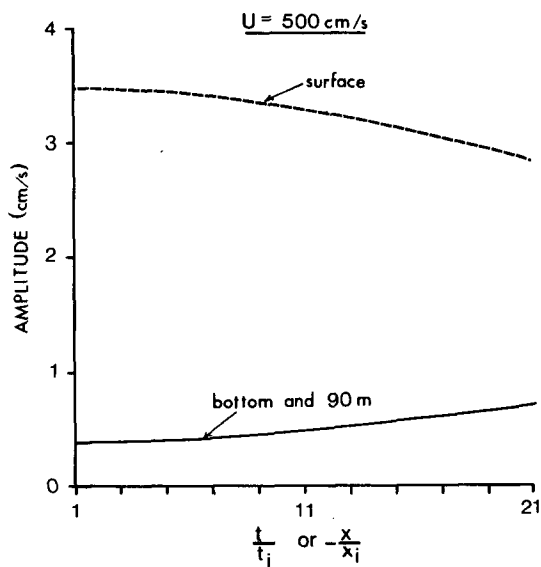


FIG. 5. Amplitude at inertial frequency due to a fast storm propagating at $U = 500$ cm s$^{-1}$. Note the depth independence of subsurface flow, and the lack of time lag for energy propagation.

Detailed maps of the positions of the northeastward propagating low pressure centers and the associated warm and cold fronts, compiled from meteorological observations, are given in the data report by Thomson and Huggett (1981b). A unique opportunity of closely tracking the position of the fronts was obtained in this experiment because of the existence of six shore based anemometer stations encircling the region of observation, shown by triangles in Fig. 6. The passage of the warm front caused a sudden veering of the wind from southeasterly to southwesterly. A map of the time lag of this veering during a mid-August event is given in Fig. 6. The front is seen to be fairly parallel to the coast, and travels northeastward at a speed of $U \sim 30$ km h$^{-1}$ = 830 cm s$^{-1}$. Since this is several times a typical $c_1$ for shelf water ($c_1 \sim 50$–$100$ cm s$^{-1}$), the expected wavelength of the oceanic response is, from (19), $\lambda \approx 2 \pi U/f \sim 500$ km, and the expected frequency is near-inertial as observed.

We shall now see whether this estimate of the wavelength agrees with the current meter data. The
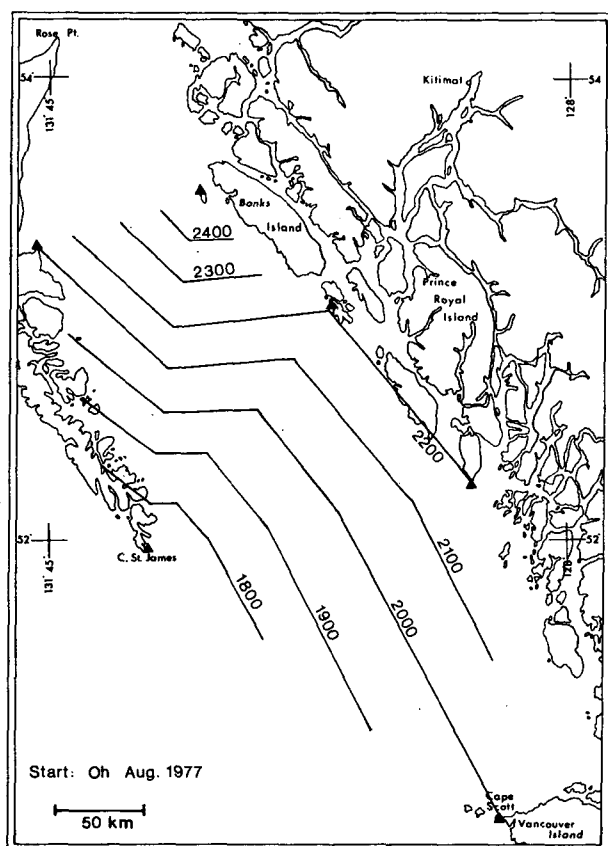
FIG. 6. Time lag of observed front propagation, determined by the time of rapid veering of winds from southeasterly to southwesterly. The data are based on six shorebased anemometer stations marked by closed triangles. Lags are in hours relative to 0000 GMT 22 August 1977.

phase differences between the currents during the mid-August event are estimated from a calculation of the complex correlation coefficient defined as (Kundu, 1976a)

$$r = \frac{\langle w_1^*(t)w_2(t)\rangle}{\langle w_1^*(t)w_1(t)\rangle^{1/2}\langle w_2^*(t)w_2(t)\rangle^{1/2}}$$

where 1 and 2 refer to the two stations, $w = u + iv$ is the complex velocity, the asterisk denotes complex conjugation, and angle brackets denotes time average. The magnitude of $r$ gives the overall measure of correlation, and the phase angle of $r$ gives the average counterclockwise angle of the second vector with respect to the first, the averaging process being weighted according to the magnitude of the instantaneous vectors. Although some of the currents are separated by several hundred kilometers, the correlations among all the currents are found to be high (larger than 0.5)—a surprising fact considering that most other observations report a lack of horizontal coherence of inertial oscillations for distances exceeding tens of kilometers.

Figure 7 shows a map of the phase difference of all the currents with respect to station QO3. The wave propagation is northeastward, and an estimate of the wavelength is $\lambda \sim 450$ km. (A similar conclusion was also reached by a complex EOF analysis, in which the first mode accounted for 71% of the energy because of the high correlation.) This is not very far from the theoretical estimate of $\lambda \sim 500$ km. The good agreement confirms that the inertial oscillations were indeed the wake of the moving front.

A similar calculation was performed for a second inertial event starting 20 June. In this case the currents were even more highly correlated in the horizontal, $r$ being as high as 0.98 for separations of order 100 km. The phase difference between the observed currents resulted in an estimate of $\lambda \sim 700$ km, but the theoretical estimate was $2\pi U/f \sim 250$ km. The agreement during this event was therefore less satisfactory.

Several other features of the solution are also in agreement with existing observations of inertial oscillations, most of which are forced by winds associated with fronts and storms. The upward phase motion in the stratified interior has been observed by Kundu (1976b), Pollard (1980) and Hamilton (1984). The multiple ("split") spectral peak associated with inertial oscillations have appeared in the observations of Kundu (1976b) and of Fu (1981; see especially his Figs. 13 and 14). The nature of the contours of $u(z, t)$ and $v(z, t)$ in the Baltic Sea observations of Krauss (1981) suggests a clear separation of the $n = 1$ mode; a split spectrum might have resulted in this case if it were computed. Short periods of slightly subinertial frequency oscillation have been observed by Kundu (1976b), and Thomson and Huggett (1981a). The
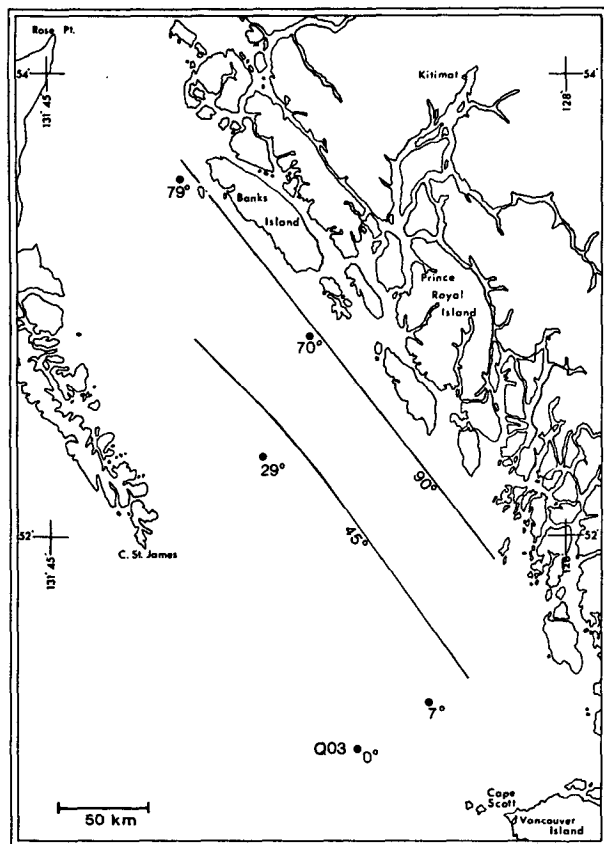
FIG. 7. Phase difference of inertial currents with respect to station QO3. The phase angle is that of the complex correlation coefficient; positive angle means that the average current is counterclockwise of that of QO3.

increase of the blue shift with depth has been observed by Millot and Crépon (1981). Intermittencies of 5–15 days duration has appeared in all observations.

## 5. Summary and remarks

Flow field due to a moving front in the form of a concentrated line source has been found. The solution for the velocity is found in terms of the vertical normal modes of the system, assuming that the ocean is inviscid, stratified, and has a flat bottom. The baroclinic solution is contained entirely behind the front, and is given by

$$u_n = -\frac{\tau_{0n}\sin k_n x}{f(1 - c_n^2/U^2)^{1/2}}, \quad k_n = \frac{f/U}{(1 - c_n^2/U^2)^{1/2}}.$$

The assumption that the front is concentrated is a good one since its thickness is much smaller than $\lambda_1$, the characteristic scale of the flow field. Perhaps the most attractive aspect of the solution is its algebraic

simplicity. Yet it contains features that illustrate the essential nature of such flow fields, and agree with the more complicated existing solutions of inertio-gravity waves. These features are:

1) The frequency is near-inertial only if $U \gg c_n$.

2) Downward energy propagation is associated with an upward phase propagation.

3) There is a continuous interchange of energy between the surface mixed layer and the stratified interior predominantly with a periodicity of $2\pi/(\omega_1 - f)$, which is the beating period of the first mode with a purely inertial oscillation (Gill, 1984).

4) The energy interchange results in an intermittency of the inertial oscillations, a universally observed fact.

5) The spectra contain multiple peaks due to the different modes. For slow storms with $U$ slightly larger than $c_1$, the peaks due to the lower modes are widely separated and distinguishable. The lowest ones of these may be noninertial waves. "Split" inertial peaks are frequently observed (Fu, 1981; Kundu, 1976b). Fast storms with $U \gg c_1$ generate oscillations that are almost exactly inertial, with little lag in the phase and energy propagation.

6) The blue shift of the primary peak increases with depth, which agrees with the observations of Millot and Crépon (1981) and the calculations of Kundu et al. (1983) and Price (1983).

7) The oscillations appear to be subinertial for short ($\sim 2t_i$) periods of time, although all modes have $\omega_n > f$. Such oscillations have frequently been observed (Kundu, 1976b; Thomson and Huggett, 1981a).

The current meter data taken off the coast of British Columbia have been analyzed. During two events forced by propagating fronts the surface inertial currents have been found to be horizontally correlated, although these currents were separated by as much as 400 km. A wavelength was estimated from the phase difference between the currents, and the relation $\lambda = Ut_i$ was found to be satisfied for one event and differed by a factor of 3 for the other event.

It has recently been shown (Kundu, 1984) that much larger inertial oscillations can be accounted for by the wind forcing than previously thought possible. Further work is therefore suggested to study wind-forced inertial oscillations. Flow field should be evaluated for a distributed source, using realistic values of the stress gradients [Eq. (8)]. The present assumption of independence perpendicular to the direction of propagation fails for occluded fronts or localized storms such as a hurricane. Geisler's (1970) horizontally bounded two-layer solution should therefore be generalized to a continuously stratified ocean.

## REFERENCES

Fu, L. L., 1981: Observations and models of inertial waves in the deep ocean. *Rev. Geophys. Space Phys.,* **19,** 141–170.

Geisler, J. E., 1970: Linear theory of the response of a two-layer ocean to a moving hurricane. *Geophys. Fluid Dyn.,* **1,** 249–272.

Gill, A. E., 1984: On the behavior of internal waves in the wakes of storms. *J. Phys. Oceanogr.,* **14,** 1129–1151.

Hamilton, P., 1984: Topographic and inertial waves on the continental rise of the Mid-Atlantic Bight. *J. Geophys. Res.,* **89,** 695–710.

Krauss, W., 1981: The erosion of a thermocline. *J. Phys. Oceanogr.,* **11,** 415–433.

Kundu, P. K., 1976a: Ekman veering observed near the ocean bottom. *J. Phys. Oceanogr.,* **6,** 238–242.

——, 1976b: An analysis of inertial oscillations observed near Oregon coast. *J. Phys. Oceanogr.,* **6,** 879–893.

——, 1984: Generation of coastal inertial oscillations by time varying wind. *J. Phys. Oceanogr.,* **14,** 1901–1913.

——, S-Y., Chao and J. P. McCreary, 1983: Transient coastal currents and inertio-gravity waves. *Deep-Sea Res.,* **30,** 1059–1082.

Millot, C., and M. Crépon, 1981: Inertial oscillations on the continental shelf of the Gulf of Lions—observations and theory. *J. Phys. Oceanogr.,* **11,** 639–657.

Pollard, R. T., 1980: Properties of near-surface inertial oscillations. *J. Phys. Oceanogr.,* **10,** 385–398.

Price, J. F., 1983: Internal wave wake of a moving storm. Part I: Scales, energy budget and observations. *J. Phys. Oceanogr.,* 949–965.

Rubenstein, D. M., 1983: Vertical dispersion of inertial waves in the upper ocean. *J. Geophys. Res.,* **88,** 4368–4380.

Thomson, R. E., and W. S. Huggett, 1981a: Wind-driven inertial oscillations of large spatial coherence. *Atmos. Ocean,* **19,** 281–306.

——, and ——, 1981b: Wind-driven inertial oscillations in Queen Charlotte Sound and Hecate Strait, May–September, 1977. Pacific Marine Science Report 81-20, Institute of Ocean Science, Sidney, B.C., 90 pp.